International Journal of Pharmaceutics 541 (2018) 214–223

Contents lists available at ScienceDirect

International Journal of Pharmaceutics

journal homepage: www.elsevier.com/locate/ijpharm

Human serum albumin nanoparticles for ocular delivery of bevacizumab

Inés Luis de Redín[a], Carolina Boiero[b], María Cristina Martínez-Ohárriz[c], Maite Agüeros[a], Rocío Ramos[d], Iván Peñuelas[d], Daniel Allemandi[b], Juan M. Llabot[b], Juan M. Irache[a,*]

[a] Department of Pharmacy and Pharmaceutical Technology, NANO-VAC Research Group, University of Navarra, Spain
[b] UNITEFA-CONICET, Department of Pharmacy, Faculty of Chemical Sciences (FCQ-UNC), National University of Córdoba, Argentina
[c] Department of Chemistry, University of Navarra, Spain
[d] Radiopharmacy Unit, Clínica Universidad de Navarra, Spain

ARTICLE INFO

Keywords:
Human serum albumin
Bevacizumab
Nanoparticles
Controlled release
Ocular delivery
Desolvation

ABSTRACT

Bevacizumab-loaded nanoparticles (B-NP) were prepared by a desolvation process followed by freeze-drying, without any chemical, physical or enzymatic cross-linkage. Compared with typical HSA nanoparticles cross-linked with glutaraldehyde (B-NP-GLU), B-NP displayed a significantly higher mean size (310 nm vs. 180 nm) and a lower negative zeta potential (−15 mV vs. −36 mV). On the contrary, B-NP displayed a high payload of approximately 13% when measured by a specific ELISA, whereas B-NP-GLU presented a very low bevacizumab loading (0.1 μg/mg). These results could be related to the inactivation of bevacizumab after reacting with glutaraldehyde. From B-NP, bevacizumab was released following an initial burst effect, proceeded by a continuous release of bevacizumab at a rate of 6 μg/h. Cytotoxicity studies in ARPE cells were carried out at a single dose up to 72 h and with repeated doses over a 5-day period. Neither bevacizumab nor B-NP altered cell viability even when repeated doses were used. Finally, B-NP were labeled with ^{99m}Tc and administered as eye drops in rats. ^{99m}Tc-B-NP remained in the eye for at least 4 h while ^{99m}Tc-HSA was rapidly drained from the administration point. In summary, HSA nanoparticles may be an appropriate candidate for ocular delivery of bevacizumab.

1. Introduction

Human serum albumin (HSA) is the most abundant protein in human blood, and is a natural and adequate material for the fabrication of nanoparticles for drug-delivery purposes. In recent decades albumin nanoparticles have gained considerable attention owing to their high capability to load a number of drugs in a non-specific way (Ghuman et al., 2005), as well as their tolerability when administered in vivo (Green et al., 2006). For the preparation of these nanocarriers a great variety of physico-chemical processes have been proposed, including thermal gelation (Qi et al., 2010; Yu et al., 2006a,b), emulsification (Crisante et al., 2009; Patil, 2003; Yang et al., 2007) and desolvation (coacervation) (Merodio et al., 2001; Weber et al., 2000; Wilson et al., 2012). In any case, desolvation-based procedures appear to be most suitable due to their simplicity and repeatability. However, the just obtained albumin nanoparticles are unstable and a supplementary step of stabilization or cross-linkage has to be performed in order to prolong their half-life in an aqueous environment and/or prevent the formation of macro-aggregates of the protein.

In general, cross-linkage with glutaraldehyde (GLU) is one of the most frequently implemented strategies to stabilize albumin nanoparticles. While it is highly effective for this purpose, the use of GLU (and other derivatives) is questionable due mainly to its toxicity and reactivity against some functional groups (e.g. primary amine residues) (McGregor et al., 2006; Van Miller et al., 2002). Thus, for the delivery of biomacromolecules (e.g. antibodies, proteins, peptides), this dialdehyde may also react with the biologically-active compound, resulting in an important loss of their activity and efficacy (Zhang et al., 2008). In addition, the potential toxicity of GLU is a concern for in vivo delivery (McGregor et al., 2006; Van Miller et al., 2002; Zhang et al., 2008). In order to overcome these drawbacks, different strategies have been proposed to harden the just formed albumin nanoparticles without the need of using toxic reagents. Amongst others, this stabilization of nanoparticles from proteins can be obtained through thermal treatment (Yang et al., 2007), high hydrodynamic pressure (Desai, 2006), enzymatic cross-linkage with genipin (Elzoghby et al., 2013; Kang et al., 2003) or transglutaminase (Huppertz and de Kruif, 2008).

Bevacizumab is a G immunoglobulin (MW of 149 kDa) composed of two 214-residue light chains and two 453-residue heavy chains that contain an N-linked oligosaccharide. This monoclonal antibody,

* Corresponding author at: Dep. Pharmacy and Pharmaceutical Technology, University of Navarra, C/ Irunlarrea, 1, 31008 Pamplona, Spain.
E-mail address: jmirache@unav.es (J.M. Irache).

https://doi.org/10.1016/j.ijpharm.2018.02.003
Received 16 December 2017; Received in revised form 31 January 2018; Accepted 4 February 2018
Available online 24 February 2018
0378-5173/

commercially available as Avastin®, targets and blocks the binding of vascular endothelial growth factor (VEGF-A) to its receptor (Weiner et al., 2010). It was approved by the FDA in 2004 for first-line treatment of metastatic colorectal cancer, and later was approved for other cancers, such as non-small-cell lung cancer and metastatic breast cancer in combination with cytotoxic chemotherapy (Gray et al., 2009; McCormack and Keam, 2008; Perren et al., 2011).

On the other hand, bevacizumab is employed off-label in the treatment of proliferative (neovascular) eye diseases, including corneal (Chang et al., 2012) and retinal neovascularization (Campochiaro, 2013), diabetic retinopathy (Arevalo et al., 2017), and age-related macular degeneration (Chappelow and Kaiser, 2008). Regarding corneal neovascularization, bevacizumab is administered as eye drops, alone (Bock et al., 2008) or in combination with other drugs such as suramin (Lopez et al., 2017). However, topical administration of bevacizumab appears to be associated with an increased risk of corneal epithelial defects that are dependent on the dose and duration of treatment (Kim et al., 2008). One possible strategy to minimize these drawbacks would be the design of nanoparticles with mucoadhesive properties, able to prolong their residence in close contact with the corneal epithelium, in order to decrease the frequency of administration and the amount of medication given. As a result, this strategy is expected to improve patient adherence as well as the safety profile and efficacy of the treatment.

The aim of this work was to prepare and characterize human serum albumin nanoparticles as carriers for ocular delivery of bevacizumab. In addition, this work also includes the evaluation of the cytotoxicity on retinal pigment epithelium cells (ARPE-19) as well as the biodistribution of the resulting nanoparticles after ocular application as eye drops in laboratory animals.

2. Materials and methods

2.1. Materials

Human serum albumin or HSA (fraction V, purity 96–99%) and glutaraldehyde (GLU) 25% aqueous solution were obtained from Sigma (Madrid, Spain). Bevacizumab (Avastin®) was purchased from Roche (Madrid, Spain). Avastin® is provided as a concentrate for solution for infusion in a single-use vial, which contains a nominal amount of either 100 mg of bevacizumab in 4 mL or 400 mg of bevacizumab in 16 mL (concentration of 25 mg/mL). The Micro BCA protein assay kit was purchased from Pierce (Thermo Fisher Scientific Inc., Illinois, USA). The Shikari Q-beva Enzyme immunoassay used for the detection of bevacizumab was purchased from Matriks Biotech (Gölbaşı, Turkey). Absolute ethanol and dimethyl sulfoxide (DMSO) were purchased from Panreac Pharma (Barcelona, Spain). All other reagents and chemicals used were of analytical grade. The cacodylate buffer, osmium tetroxide and uranyl acetate were purchased from Sigma–Aldrich (St Louis, USA). Formvar® films were purchased from Agar Scientific (Stansted, UK). Dubelcco's modified Eagle's medium (DMEM; Sigma–Aldrich, St Louis, MO, USA), phosphate buffered saline (PBS), fetal bovine serum (FBS), fungizone and L-glutamine penicillin-streptomycin (Invitrogen) were purchased from Thermo Fisher Scientific Inc. (Illinois, USA). MTT (3-[4,5-dimethylthiazol-2-yl]-2,5 diphenyltetrazolium bromide) was provided by Sigma-Life Science (Mannheim, Germany). Acuolens® eye drops were purchase from Alconcusí (Barcelona, Spain). Tin-chloride dihydrate and chlorhydric acid were supplied by Panreac (Barcelona, Spain).

2.2. Preparation of human serum albumin nanoparticles with GLU (NP-GLU)

Human serum albumin (HSA) nanoparticles were prepared by a desolvation method as previously described (Merodio et al., 2001) with some modifications. Briefly, 100 mg of HSA was dissolved in 7.5 mL purified water and the solution was titrated to pH 4.9 with HCl 1 M. Then, nanoparticles were formed by the continuous addition of 16 mL ethanol under magnetic stirring. After the desolvation process, nanoparticles were cross-linked with GLU (12.5 µg glutaraldehyde in 300 µL ethanol) by incubation under stirring for 5 min. The organic solvents were eliminated under reduced pressure (Büchi Rotavapor R-144; Büchi, Postfach, Switzerland) and the nanoparticle suspension was purified twice by centrifugation at 41,000*g* for 20 min at 4 °C (Sigma 3 K30 Osterodeam Harz, Germany). Finally, the nanoparticles were freeze-dried (Genesis 12EL, Virtis, NewYork, USA) using a 5% sucrose solution as a cryoprotector.

2.3. Preparation of bevacizumab-loaded nanoparticles

For the preparation of bevacizumab-loaded nanoparticles, the monoclonal antibody was added to an aqueous solution containing 100 mg HSA, adjusted to a pH 4.9 with HCl 1 M, and incubated for 10 min. Then, nanoparticles were obtained by the continuous addition of 16 mL ethanol under magnetic stirring. The organic solvents were eliminated under reduced pressure (Büchi Rotavapor R-144; Büchi, Postfach, Switzerland) and the resulting suspensions were purified and freeze-dried as described above. This formulation was identified as B-NP.

As control, bevacizumab-loaded nanoparticles cross-linked with glutaraldehyde (B-NP-GLU) were also prepared. For this purpose, the just formed bevacizumab-loaded nanoparticles were incubated with 12.5 µg glutaraldehyde for 5 min at room temperature. Then, these nanoparticle suspensions were purified and freeze-dried as described above.

2.4. Physico-chemical characterization of nanoparticles

2.4.1. Size, zeta potential and morphology

The particle size and zeta potential of loaded or empty HSA nanoparticles were determined by photon correlation spectroscopy (PCS) and electrophoretic laser Doppler anemometry, respectively, using a Zeta Plus analyzer system (Brookhaven Inst. Corp., NY, USA). The diameter of the nanoparticles was determined after dispersion in ultrapure water (1/10) and measured at 25 °C by dynamic light scattering angle of 90 °C. The zeta potential was determined as follows: 200 µL of the samples were diluted in 2 mL of a 0.1 mM KCl solution adjusted to pH 7.4.

The morphological characteristics of the nanoparticles were studied by transmission electron microscopy (TEM) using copper grids covered with Formvar film for negative staining. Then, 5 µL of each sample were absorbed to the grid for 30 s, followed by washing with Milli-Q water (3 times). Samples were then exposed to 2% uranyl acetate solution in water for 5 min. After removing excess stain with filter paper, the samples were air-dried and examined at 80 kV on a Zeiss Libra 120 transmission electron microscope (Stuttgart, Germany).

2.4.2. Yield

The amount of protein transformed into nanoparticles was calculated by micro-BCA analysis and microfluidic electrophoresis. Briefly, 10 mg of the nanoparticles were dispersed in 10 mL of ultra-pure water and centrifuged at 21,000*g* for 15 min at 4 °C (Biofuge Heraeus, Hanau, Germany). Then, the pellet was digested with 1 mL of 0.02 N NaOH and the mixture centrifuged. Samples of these supernatants were analyzed with the Protein Assay Reagent Kit (Pierce, Rockford, USA), following the manufacturer's instructions.

In parallel, for bevacizumab-loaded nanoparticles, the amounts of albumin and monoclonal antibody were calculated by microfluidic electrophoresis in an Experion™ Automated Electrophoresis System (Bio Rad, Hercules, USA). Again, samples from supernatants in 0.02 N NaOH were treated in non-reducing conditions following the manufacture's specification (Experion System Pro260 Analysis Kit; Bio-Rad Lab.,

Hercules, USA). Data were processed using the Experion™ software. A virtual gel with densitometric bands expressed in kilodaltons (kDa) and the percentage of total protein (% total) value for each detected peak were obtained.

2.4.3. Bevacizumab integrity studies

The integrity of bevacizumab encapsulated in HSA nanoparticles was studied through microfluidic-based automated electrophoresis using an Experion™ Automated Electrophoresis System (Bio Rad, Hercules, USA). For this purpose, nanoparticles were broken with 1 mL NaOH 0.02 N and the samples diluted with purified water to obtain a protein concentration of around 400 ng protein/μL (linear dynamic range of the test is 5–2000 ng/μL). Samples of free protein (albumin and bevacizumab) were used as controls. The analysis was performed under non-reducing conditions as described above.

2.4.4. Quantification of bevacizumab

The amount of the antibody loaded in albumin nanoparticles was calculated by a specific enzyme immunoassay for bevacizumab (Shikari Q-BEVA). For this purpose, 10 mg of the nanoparticles were dispersed in 1 mL water and centrifuged for 10 min at 21,000*g* (Biofuge Heraeus, Hanau, Germany). The supernatant was removed and the pellet was broken with 1 mL NaOH 0.02 N. Samples were diluted 1:1000 with assay buffer and 25 μL of the resulting solution was transferred to a 96-well microplate coated with human vascular endothelial growth factor (VEGF) and followed a specific ELISA for bevacizumab (Q-Beva test procedure, Shikari Q-Beva, Matriks Biotek, Ankara, Turkey). Empty nanoparticles were treated in the same way to rule out any interference.

All samples were assayed in triplicate and the calculations performed using standard curves in the range 0.1–100 μg/mL ($r^2 > 0.993$). The detection and quantification limits were lower than 30 ng/mL and 100 ng/mL, respectively. The results were expressed as the amount of bevacizumab (μg) per mg nanoparticles (payload) and as encapsulation efficiency (in percentage).

2.4.5. FTIR determinations

The molecular structure of nanoparticles was investigated by attenuated total reflectance infrared spectroscopy (FTIR-ATR), using a Nicolet Avatar 360 spectrometer (Artisan Technology Group, Champaign, USA) equipped with a Golden-Gate temperature controlled. Samples were placed directly on the diamond and the spectra collected over 600–4000 cm^{-1} at 2 cm^{-1} resolution and 100 scans per spectrum. For the analysis of glutaraldehyde, the reagent was previously lyophilized in a Genesis 12EL lyophilizer. In all cases data were analyzed using the OMNICTM software (Thermo Fisher Scientific, Madison, USA).

2.4.6. X-ray diffraction studies

X-ray studies were performed in order to study the crystalline state of the polymeric matrix in the different samples of nanoparticles. For this purpose, the samples were placed in powder form on a plastic plate in a diffractometer (Bruker Axs D8 Advance, Frankfurt, Germany) using a Ni filter, CuKa radiation, a voltage of 40 kV and a current of 30 mA. The scanning rate was 1°/min and the time constant 3 s/step over a 2q interval of 2-40°. For the analysis of glutaraldehyde, the reagent was previously lyophilized in a Genesis 12EL apparatus. In all cases the diffractograms were analyzed using the program Diffrac.Suite software (Bruker Corp., Frankfurt, Germany).

2.4.7. Thermal analysis

The response of the different nanoparticles to heating was studied by differential thermal analysis (DTA) using a TGA/sDTA 851e Mettler Toledo thermal analyzer. (Mettler Toledo, Port Melbourne, Australia). The thermograms were obtained by heating about 5–10 mg of the sample in a pierced aluminum crucible at a scan rate of 10 °C/min from 25 to 250 °C. The thermal analyses were performed under static air atmosphere using 20 mL min^{-1} nitrogen as purge gas. Measurements were made in triplicate. Again, glutaraldehyde was lyophilized before use.

2.4.8. Elemental analysis

Elemental analysis (C, H, O and N) of the nanoparticles was performed in order to confirm the association of the different stabilizing agents in the HSA nanoparticles using an Elemental Analyzer from LECO (CHN-900, Michigan USA). Briefly, 1 mg of each sample was tested in triplicate and results were expressed as a percentage (% w/w) SD ± 0.4.

2.5. Stability of nanoparticles

The stability of nanoparticles was evaluated in phosphate buffered saline medium (PBS, pH 7.4). Nanoparticles were dispersed in this solution and stored at room temperature for a period of 24 h. At predetermined times, the stability was assessed by measuring the size, polydispersity and zeta potential of the nanoparticles.

2.6. In vitro release study

In vitro release profile of bevacizumab from albumin nanoparticles were carried out in PBS (pH 7.4). Due to the eventual aggregation of bevacizumab in PBS, we selected an appropriate dilution factor to prevent this phenomenon. For this purpose, aggregation of bevacizumab was evaluated after dissolving the monoclonal antibody in PBS by electrophoresis. After this preliminary study, eppendorf tubes containing 10 mg of each formulation (B-NP-GLU and B-NP) were dispersed in 1 mL PBS and placed in a shaking bath at 37 °C with a constant agitation of 60 S/min (Vortemp 56, Labnet International, Woodbridge, USA). At different times, samples were centrifuged for 10 min at 21,000*g* (Biofuge Heraeus, Hanau, Germany), and the supernatants were analyzed for bevacizumab content with the specific ELISA test (Shikari Q-Beva, Matriks Biotek, Ankara, Turkey). The analysis was performed three times for each sample. Release profiles were expressed in terms of cumulative release in percentage, and plotted versus time.

2.7. Cell culture

ARPE19 were employed in this study as a model of ocular epithelial cells. Cells were grown to confluence in DMEM medium, containing 10% FBS, 1% fungizone, 1% L-glutamine-penicillin–streptomycin. Cells were cultured in a humidified incubator containing 5% CO2 at 37 °C.

Cell suspensions were seeded onto 96-well tissue culture plates, starting at an initial concentration of 5×10^3–1×10^4 cells/mL. After 24 h, culture medium was replaced by the different nanoparticle formulations diluted to the desired final concentration (0.0, 0.1, 0.5, 1.0, 1.5 and 2.0 mg/mL) with culture medium and tested for up to 72 h.

2.7.1. MTT toxicity assay

To evaluate the effect of bevacizumab (free or encapsulated as B-NP) on ARPE19 cells, cell proliferation was determined by using the MTT (3-(4,5-dimethylthiazol-2-yl)-2,5-diphenyltetrazoliumbromide) assay. ARPE19 cells (5×10^3–1×10^4 cells/mL) were plated into 96-well microtiter plates (Nunc, Thermo Fisher, Scientific Inc., Illinois, USA). After 24 h, plates were washed with PBS and culture medium replaced with bevacizumab preparations dispersed in fresh medium. Cells were then incubated for 4, 24 or 48 h, culture media removed and 250 μL of 0.5 mg/mL MTT added to the cells during 4 h (37 °C, 5% CO2, 95% humidified air). Then, 200 μL of dimethyl sulfoxide (DMSO) was added to extract the reduced formazan produced by living cells, and cellular viability measured by quantifying it by colorimetry analysis at 540 nm.

On the other hand, the effect of repeated doses of bevacizumab on

cellular viability was also evaluated. For this purpose, ARPE-19 cells were exposed to the following two bevacizumab regimens: (i) every other day (days 0, 2, and 4) and (ii) daily at days 0, 1, 2, 3, and 4. In both cases, the MTT assay was performed at day 5 as described above.

2.8. Radiolabelling of nanoparticles and biodistribution study in animals

Albumin nanoparticles (B-NP) were radiolabeled with ^{99m}Tc by reduction with tin chloride following a previously described method (Sánchez-Martínez et al., 2013). Briefly, 40 µL of a 0.02 mg/mL tin chloride dihydrate solution in water for injection at pH 4 (adjusted with HCl 0.1 N) were mixed with 0.5 mg of lyophilized nanoparticles. After this, 200 µL of ^{99m}TcO4− eluate from a ^{99}Mo/^{99m}Tc generator (Ultratechneflow™, Mallinkrodt, The Netherlands) were added to the mixture. For in vivo studies, 4 µL of the radiolabelled nanoparticle suspension (40 MBq) were mixed with 1.75 mg of unlabelled B-NP formulation.

For ^{99m}Tc-labelled albumin controls, 5 µL of a 20 mg/mL albumin solution where labelled with 200 µL of ^{99m}TcO4 − eluate and 40 µL of 0.05 mg/mL tin chloride dihydrate solution. Just before use, 4 µL of radiolabelled albumin were mixed with 4 µL of a commercial collyrium (Acuolens®) containing 3 mg/mL hydroxypropyl methylcellulose.

For the biodistribution study, experiments were performed in compliance with the regulation of the Ethics Committee of the University of Navarra in line with the European legislation on animal experiments (protocols 171-12 and 066/16). For this purpose, female Wistar rats (250 g) were anesthetized with isoflurane and received 4 µL of the radiolabelled formulation on the right eye. Animals were kept anesthetized for one hour to avoid active removal of the suspension from the eye.

The following treatments were evaluated: (i) radiolabelled nanoparticles (5 MBq; ^{99m}Tc-B-NP), (ii) radiolabelled albumin in the commercial collyrium (4 MBq; ^{99m}Tc-HSA), and (iii) ^{99m}TcO4 − eluate in the collyrium (5 MBq; ^{99m}Tc-free). For imaging studies, animals where anesthetized just before each study and placed in prone position in a Symbia T2 Truepoint SPECT-CT system (Siemens). Images were acquired using a 128 × 128 matrix, 7 images/s. CT was set to 110 mAs and 130 kV, 130 images 3 mm thick. Image fusion was performed using Syngo MI Applications TrueD software.

2.9. Statistical analysis

Data are expressed as the mean ± S.D of at least three experiments. The data obtained were statistically treated by variance analysis, while the means were compared by one way ANOVA at a significance level of 0.05. All calculations were performed using GraphPad Prism 6.0 statistical software (GraphPad Software, CA, USA).

3. Results

3.1. Preparation and characterization of nanoparticles

Albumin nanoparticles prepared by a desolvation process of the protein in water after addition of ethanol showed low stability in an aqueous environment and were stabilized by cross-linkage with glutaraldehyde. The resulting nanoparticles had a mean size of about 165 nm and a negative zeta potential of −36 mV (Table 1).

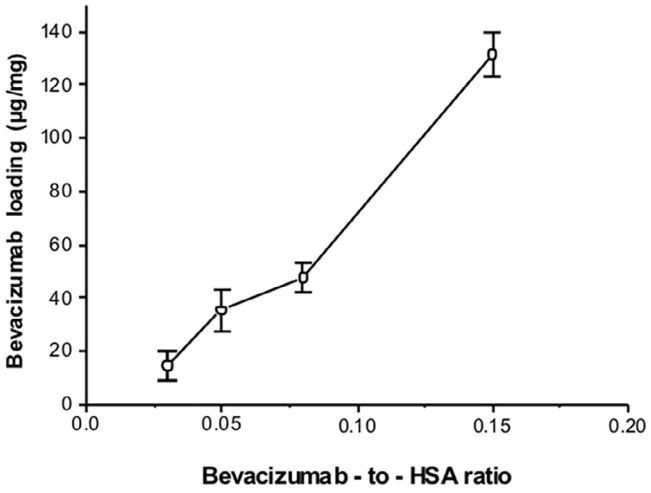

Fig. 1. Influence of the bevacizumab-to-albumin ratio on the payload of the resulting nanoparticles. Data expressed as mean ± SD (n = 3).

For optimization of the bevacizumab-loaded nanoparticles, the influence of the antibody-to-albumin ratio on the payload was evaluated (Fig. 1). When the bevacizumab-to-albumin ratio was low (e.g. 0.01), the resulting nanoparticles were not stable with time and needed to be cross-linked with glutaraldehyde. However, for ratios higher than 0.01, bevacizumab-loaded nanoparticles were stable with no need for a supplementary stabilization step. In addition, the payload of the resulting nanoparticles increased by augmenting the antibody-to-albumin ratio up to 0.15. Under these experimental conditions, the resulting nanoparticles (B-NP) displayed a mean size close to 300 nm and a negative zeta potential of about −15 mV. Moreover, bevacizumab loading was calculated to be close to 13%, with an encapsulation efficiency of about 90% (Table 1). The integrity of bevacizumab entrapped in albumin nanoparticles was evaluated by microfluidic-based automated electrophoresis (Fig. 2).

Interestingly, when these bevacizumab-loaded nanoparticles were cross-linked with glutaraldehyde (B-NP-GLU), the mean size was significantly lower than those non-stabilized with the dialdehyde (180 vs. 310 nm), and their negative zeta potential was also significantly lower (-36 mV vs. −14 mV). In both cases, the polydispersity index (PDI) was found to be lower than 0.2, indicating homogeneous nanoparticle formulations. Regarding the payload for B-NP-GLU, the antibody loading was of only 0.1 µg/mg nanoparticle (Table 1).

Fig. 2 shows a microfluidic electrophoresis analysis of B-NP. By this technique, both HSA and bevacizumab appeared as strong bands at about 65 and 150 kDa, respectively. Likely, the formation of nanoparticles did not significantly alter the structural integrity of bevacizumab.

The morphological evaluation of nanoparticles by transmission electron microscopy (TEM) revealed some differences when nanoparticles were cross-linked with glutaraldehyde (Fig. 3). Thus, NP-GLU

Table 1
Physical-chemical characteristics of empty and bevacizumab-loaded nanoparticles Data are expressed as mean ± SD, n = 3. NP: empty and non-hardened nanoparticles; B-NP: bevacizumab-loaded nanoparticle not treated with glutaraldehyde; NP-GLU: empty nanoparticles treated with glutaraldehyde; B-NP-GLU: bevacizumab-loaded nanoparticles cross-linked with glutaraldehyde.

Formulation	Size (nm)	PDI	Zeta potential (mV)	Yield (%)	EE (%)	BEVA loading (µg/mg NP)
NP	NA	NA	NA	NA	–	–
B-NP	310 ± 3	0.14 ± 0.02	−14 ± 1	85 ± 3	89 ± 0	132 ± 5
NP-GLU	163 ± 2	0.17 ± 0.01	−36 ± 0	66 ± 5	–	–
B-NP-GLU	180 ± 3	0.11 ± 0.01	−36 ± 1	75 ± 2	0.1 ± 1.3	0.1 ± 1

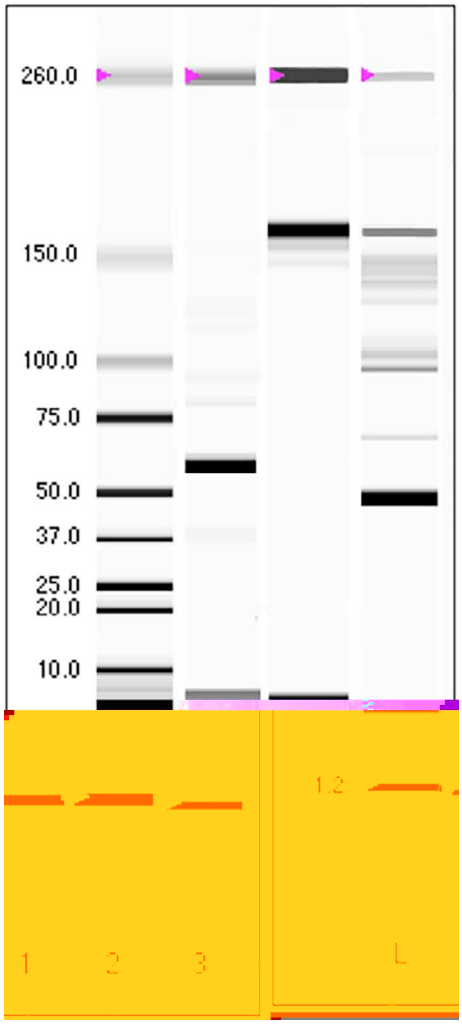

Fig. 2. Microfluidic-based automated electrophoresis of nanoparticles (L: Ladder; 1: HSA; 2: BEVA; 3: B-NP).

(Fig. 3A) and B-NP-GLU (Fig. 3B) were spherical and with a well-defined perimeter. On the contrary, B-NP (Fig. 3C) presented an irregular contour.

Fig. 4 shows the FTIR spectra of the different compounds employed in the preparation of nanoparticles as well as those of the resulting nanocarriers. In case of nanoparticles cross-linked with glutaraldehyde (NP-GLU), the typical band of the dialdehyde (1690 cm^{-1}) was not observed. In a similar way, no displacement of the amide bands I and II (1644 cm^{-1} and 1533 cm^{-1}, respectively) of albumin was detected in the spectra corresponding to NP-GLU, B-NP-GLU or B-NP. However, a change in the relative intensity of those bands (corresponding to amides I and II) was evidenced when compared with the typical spectrum of HSA (Fig. 4). Furthermore, a broadening of the amide I band in the spectra of nanoparticle formulations was also identified.

The effect of bevacizumab encapsulation and glutaraldehyde treatment was also evaluated by X-ray diffraction. Fig. 5 shows these results. In all cases, X-ray diffractograms displayed patterns corresponding to amorphous structures. It is worthy to note that for nanoparticles cross-linked with glutaraldehyde (NP-GLU and B-NP-GLU), the diffraction patterns presented a similar profile to that of the dialdehyde.

Fig. 6 shows the thermograms of albumin, glutaraldehyde, bevacizumab and the resulting nanoparticles. HSA showed an exothermic effect around 30 °C, corresponding to a reversible conformational change, and a second endothermic band (at 80 °C) due to protein unfolding processes that take place by heating. Glutaraldehyde presented a weak endothermic effect at around 180 °C that could correspond to a

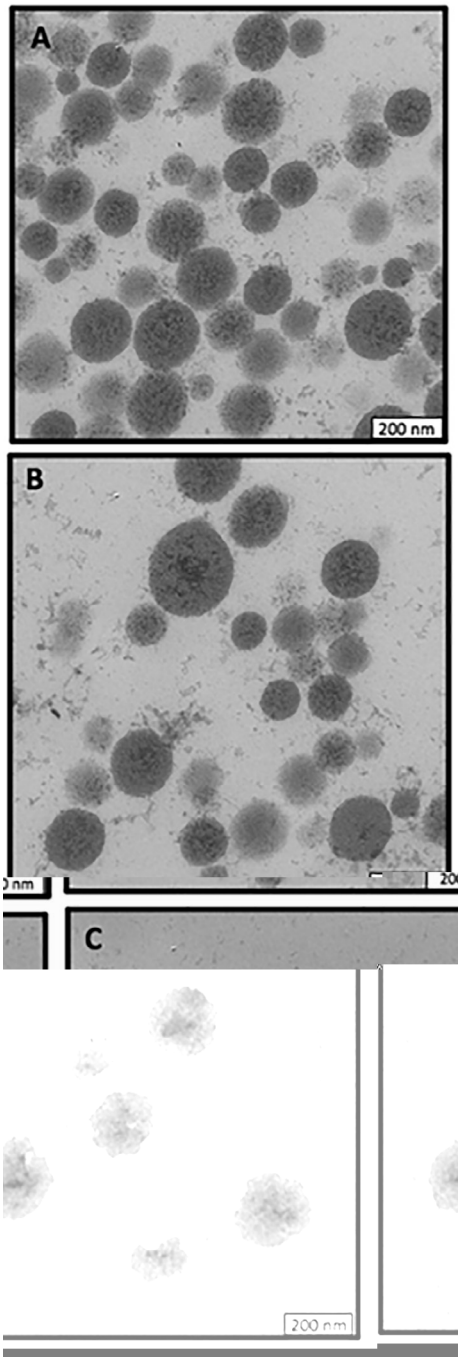

Fig. 3. TEM microphotographs of nanoparticles. A: empty nanoparticles cross-linked with glutaraldehyde (NP-GLU). B: bevacizumab-loaded nanoparticles cross-linked with glutaraldehyde (B-NP-GLU). C: bevacizumab-loaded nanoparticles not treated with glutaraldehyde (B-NP).

fusion process (for this study glutaraldehyde employed in a solid form after freeze-drying). Bevacizumab showed a broad endothermic band that would be associated to its denaturation process. It is noteworthy that, for nanoparticle samples, no thermal signals corresponding to HSA were observed. This fact could be attributed to the interaction between albumin and the monoclonal antibody when the nanoparticles are formed. In addition, a certain drift of the thermal profile can be associated to changes in the thermal diffusivity of the nanoparticles with respect to the mixture of components.

Table 2 shows the elemental analysis of the nanoparticles employed in this study as well as of the three individual components (human serum albumin, bevacizumab and glutaraldehyde). Comparing both

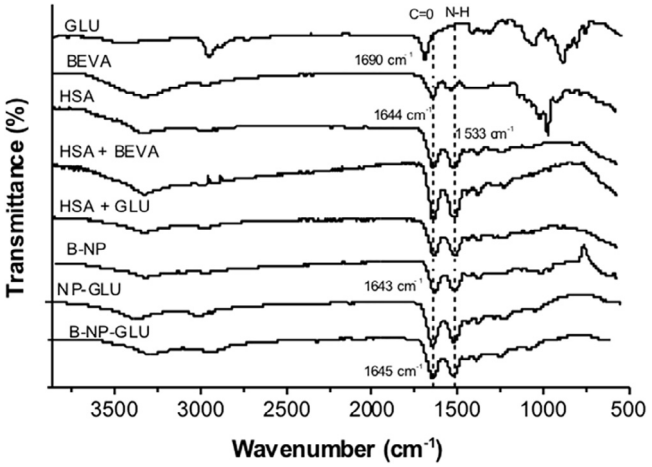

Fig. 4. FTIR Spectrum of glutaraldehyde (GLU), bevacizumab (BEVA), human serum albumin (HSA), HSA + BEVA physical mixture, HSA + GLU physical mixture, BEVA-loaded albumin nanoparticles (B-NP), albumin nanoparticles cross-linked with glutaraldehyde (NP-GLU) and BEVA-loaded albumin nanoparticles cross-linked with glutaraldehyde (B-NP-GLU).

proteins, bevacizumab displayed a significantly lower content of carbon and nitrogen than human serum albumin. On the contrary, the oxygen content in the monoclonal antibody was about 2-times higher than in albumin. For glutaraldehyde, the most important points were the lack of nitrogen and the presence of significant oxygen content (about 50%). On the other hand, albumin nanoparticles containing bevacizumab (B-NP-GLU and B-NP), presented a lower percentage of nitrogen and higher oxygen content than native albumin. Also, empty nanoparticles cross-linked with GLU showed higher amounts of oxygen and lower amounts of nitrogen as compared with native albumin.

3.2. Stability of nanoparticles

Fig. 7 shows the evolution of the mean size of nanoparticles when incubated in either PBS (Fig. 7A) or cell culture medium (Fig. 7B) for 24 h. No significant changes in the mean size were observed for any of the nanoparticles (NP-GLU, B-NP-GLU and B-NP) during the following 24 h. On the other hand, for all the nanoparticles tested, no significant changes in the zeta potential or polydispersity values were evidenced during the experiment (data not shown).

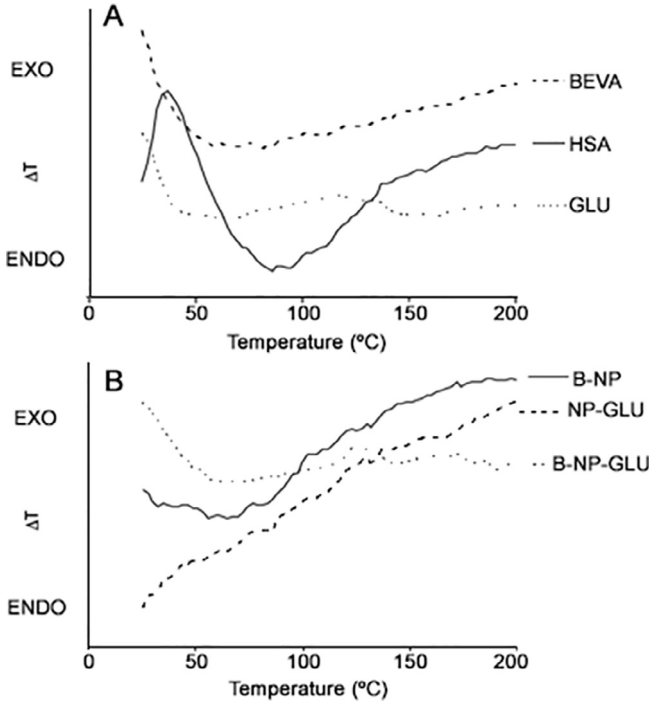

Fig. 6. DTA thermograms of (A) native albumin (HSA), bevacizumab (BEVA) and glutaraldehyde (GLU) and (B) albumin nanoparticles cross-linked with glutaraldehyde (NP-GLU), bevacizumab-loaded nanoparticles (B-NP) and bevacizumab-loaded nanoparticles coated with glutaraldehyde (B-NP-GLU).

Table 2
Elemental analysis of albumin (HSA), glutaraldehyde (GLU), bevacizumab (BEVA), albumin nanoparticles cross-linked with glutaraldehyde (NP-GLU), bevacizumab-loaded nanoparticles (B-NP) and bevacizumab-loaded nanoparticles cross-linked with glutaraldehyde (B-NP-GLU).

	% C	% H	% N	% O
HSA	48.34	6.96	17.80	26.91
GLU	42.84	6.29	0.23	50.63
BEVA	36.70	6.64	4.25	52.41
NP-GLU	48.09	6.87	15.19	29.85
B-NP	48.77	6.86	14.90	29.48
B-NP-GLU	49.27	6.70	14.61	29.42

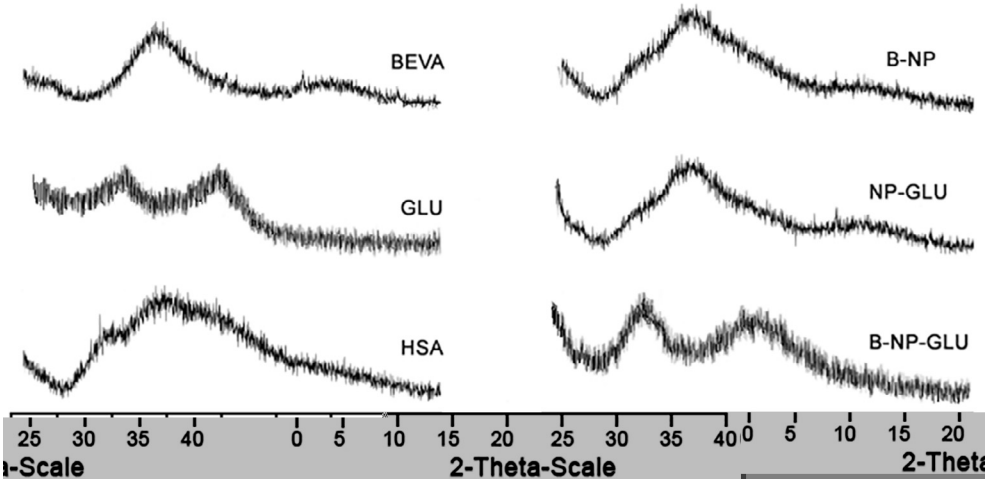

Fig. 5. X-ray spectra of albumin, bevacizumab, glutaraldehyde and the different nanoparticles used in this study.

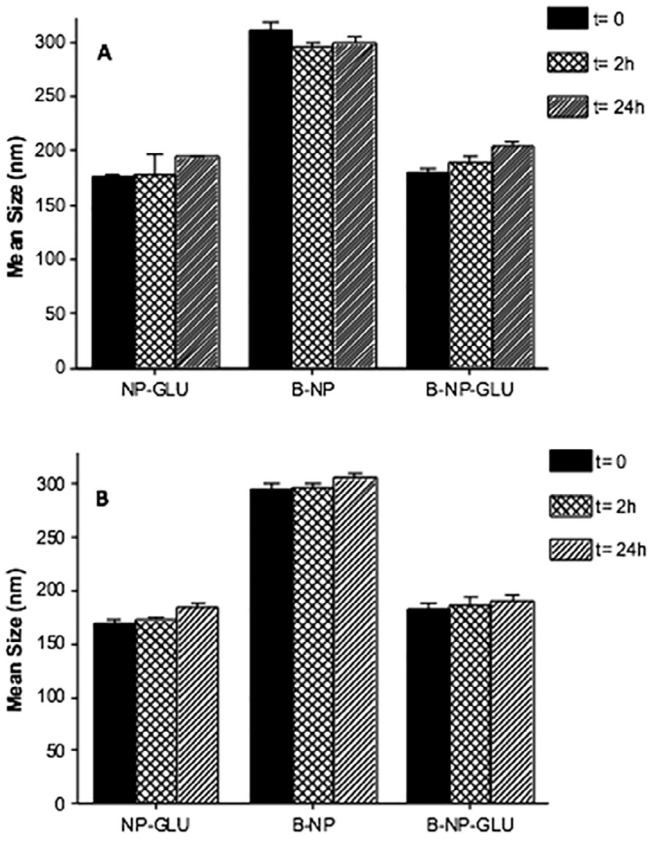

Fig. 7. Evolution of the mean size of empty nanoparticles cross-linked with glutaraldehyde (NP-GLU) and bevacizumab-loaded nanoparticles (B-NP and B-NP-GLU) after their dispersion in either PBS at pH 7.4 (A) or DMEM (B). Data expressed as mean ± SD, n = 3.

3.3. In vitro release studies

Fig. 8 shows the in vitro release profile of bevacizumab from albumin nanoparticles (B-NP) in PBS at pH 7.4. These nanoparticles presented a biphasic release pattern characterised by an initial release (burst effect) of about 400 µg/mL (35% of the loaded bevacizumab) in the first 5 min, followed by a slower, more sustained release rate during at least 24 h, up to 500 µg/mL. Therefore, the release profile obtained could not be adjusted to any mathematical model. B-NP-GLU was not evaluated due to the very low amount of active bevacizumab released to the dissolution medium (less than 1%).

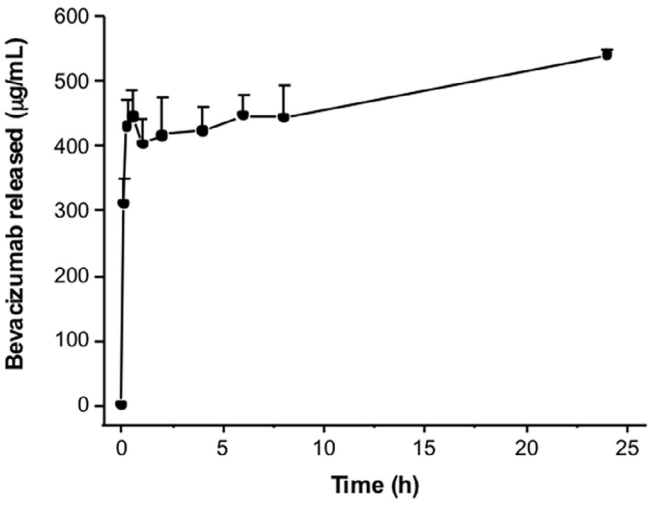

Fig. 8. Bevacizumab release profile from albumin nanoparticles (B-NP) after incubation in PBS (pH 7.4). Data expressed as mean ± SD, n = 3.

3.4. Cell culture experiments

None of the cell proliferation assays carried out at for up to 72 h after one single dose of bevacizumab (either free or loaded in albumin nanoparticles showed important changes in the cell viability rate of ARPE cells (Fig. 9). Only, at the lowest concentrations tested (0.1 and 0.5 mg bevacizumab per mL), an increase on cell proliferation was observed.

ARPE cells treated with repeated doses of bevacizumab also showed a low influence on the viability of cells (Fig. 10). Only treatment with free bevacizumab every other day over a 5-day period induced a slight decrease on cellular proliferation (Fig. 10A).

3.5. Ophthalmic administration to Wistar rats for in vivo SPECT-CT imaging

Fig. 11 shows the biodistribution of B-NP after ocular administration as eye drops. Radioactivity associated with bevacizumab-loaded nanoparticles (^{99m}Tc-B-NP) remains in the eye for at least 4 h, and progressively disappeared from the administration point into the GI tract. On the other hand, free ^{99m}TcO4- and ^{99m}Tc-HSA incorporated in the commercial collyrium, showed a short residence time on the eye. This was particularly evident for ^{99m}Tc-HSA. Thus, 1 h after its administration as eye drops, the majority of the radioactivity was visualized in the gut of animals (Fig. 11B).

4. Discussion

Human serum albumin is a 66 kD protein abundantly present in plasma that is widely employed as pharmaceutical excipient for different applications. Its high stability in liquid media and amphiphilic properties makes it suitable in the formulation of many therapeutic proteins, as additive to minimize irreversible adsorption to the container or aggregation phenomena (Bouyer et al., 2012; Sadaharu et al., 2004). HSA, due to its high glass transition temperature, can be employed as cryoprotectant in freeze-drying processes (Hawe and Friess, 2006). Moreover, HSA is also employed as material for the preparation of micro- and nanoparticles such as Albunex® (Christiansen et al., 1994) or Abraxane® (Ibrahim et al., 2002).

In addition to its safety and regulatory acceptation, HSA offers a supplementary advantage that is related with its remarkable capability to bind a high variety of drugs (Fasano et al., 2005; Kratz, 2008). The preparation of HSA nanoparticles is relatively easy and, in general, can be performed under mild conditions (Kouchakzadeh et al., 2014; Langer et al., 2008). However, the formed nanoparticles are not sufficiently stable and they dissolve after dispersion in water (Niknejad and Mahmoudzadeh, 2015; Weber et al., 2000). Therefore, a stabilization step is required. The most common strategy to stabilize HSA-based nanoparticles is cross-linkage with glutaraldehyde as its aldehyde groups easily react with albumin amino groups resulting in stable particles. However, its use is controversial due to the potential toxicity of glutaraldehyde and also because it could potentially react with the amino groups of the encapsulated drug (Langer et al., 2008; McGregor et al., 2006; Merodio et al., 2001). In this context, our first approach was to look for “soft” cross-linking procedures, such as the combination of ultraviolet irradiation and glucose (Niknejad and Mahmoudzadeh, 2015). Nevertheless, the encapsulation of bevacizumab in HSA (B-NP) yielded stable nanoparticles without the need of any “hard” method. This fact may be explained by the development of protein-protein interactions between the monoclonal antibody and albumin (Fan et al., 2017; Son et al., 2013; Yang et al., 2014). Likely, in our case and under the experimental conditions described here, these interactions would result in nanoparticles as stable submicron assemblies (B-NP). This idea

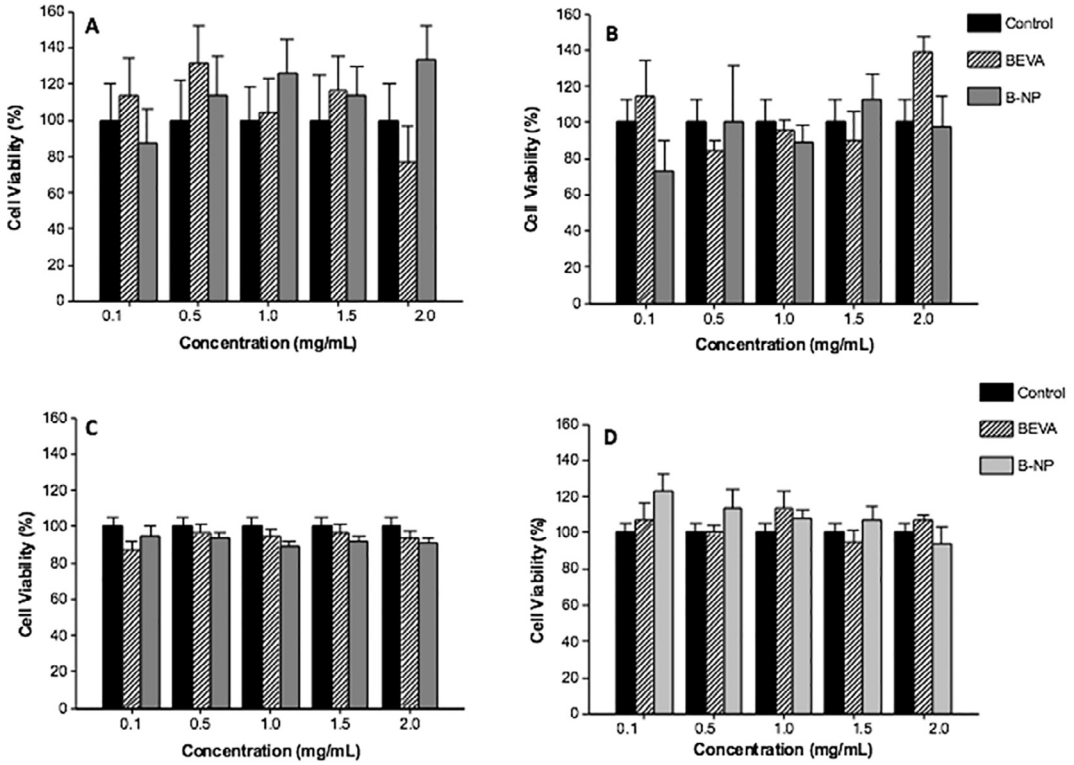

Fig. 9. Single dose MTT assay following incubation of nanoparticles with ARPE cells for 4 h (A), 24 h (B), 48 h (C) or 72 h (D). The results are expressed as mean ± SD, n = 6.

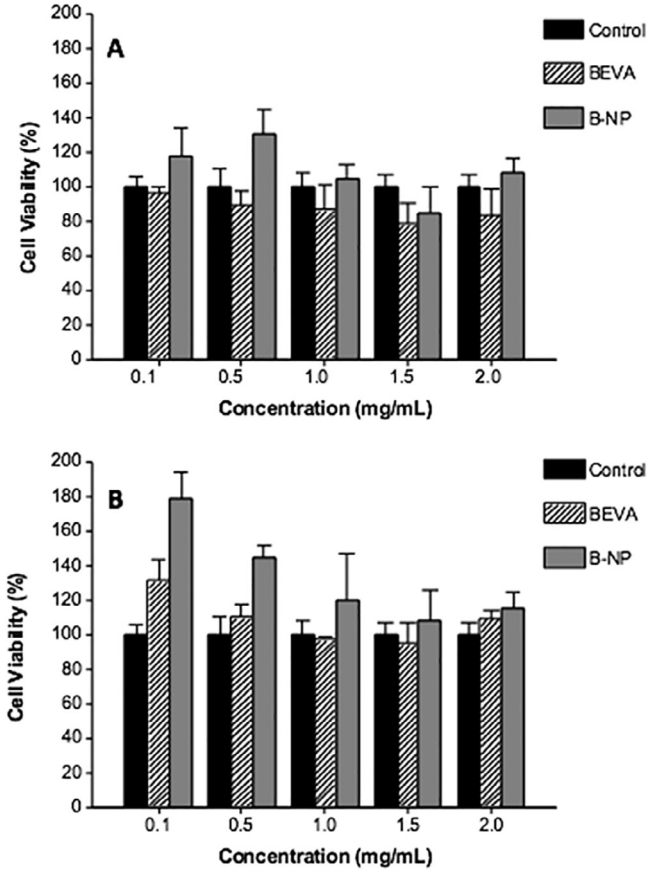

Fig. 10. Repeated dose MTT assay following treatment either every over day (A) or every 24 h (B) over a 5-day period. The results are expressed as mean ± SD, n = 3.

is supported by IR analysis, in which changes in the relative intensity of amide I (C═O stretch) and amide II (C−N stretch coupled with N−H bending mode) bands were observed. These modifications would be related with the formation of hydrogen bonds between C═O and N−H functional groups in bevacizumab and albumin (Ahmed et al., 2013). In addition, changes in the typical fingerprint of bevacizumab (around 1000 cm^{-1}) for loaded nanoparticles were also detected. Another evidence of the interactions between albumin and bevacizumab in B-NP was obtained by DTA analysis (Fig. 6). Contrary to the thermal signals observed for bevacizumab (endothermic band at 70 °C) or native albumin (exothermic peak at 30 °C and endothermic unfolding process at 80 °C) no relevant peaks were observed when B-NP was evaluated. In a similar way, elemental analysis corroborated the different composition of bevacizumab-albumin assemblies when compared with the different compounds employed in their preparation (Table 2). Thus, compared with albumin, the incorporation of bevacizumab in nanoparticles produced an increase in the amount of oxygen and a decrease in the amount of nitrogen.

These submicronic aggregates of bevacizumab and albumin (B-NP) showed a significantly higher mean size than glutaraldehyde cross-linked nanoparticles (310 nm vs. 180 nm for B-NP-GLU) as well as a significantly lower negative zeta potential (−14 mV for B-NP vs. −36 mV for B-NP-GLU). From a morphological point of view, B-NP were also different to B-NP-GLU (Fig. 3). In addition, our preparative process of B-NP resulted in high payloads (13.2%) of active bevacizumab (as determined by ELISA, see Table 1). These values are in line with those previously published for PLGA and PEG-PLA nanoparticles (Li et al., 2012; Sousa et al., 2017) and are significantly higher than other obtained with solid lipid nanoparticles (Battaglia, 2010) or nanoliposomes (Abrishamid et al., 2009). When incubated in PBS, bevacizumab was released from albumin nanoparticles following a biphasic profile (Fig. 8). In the first step, an important amount of the loaded bevacizumab (about 30%) was rapidly released following a burst effect, while in the second step a continuous amount of the monoclonal antibody was released over time (around 6 μg/h).

Furthermore, B-NP did not produce alterations in cell viability even

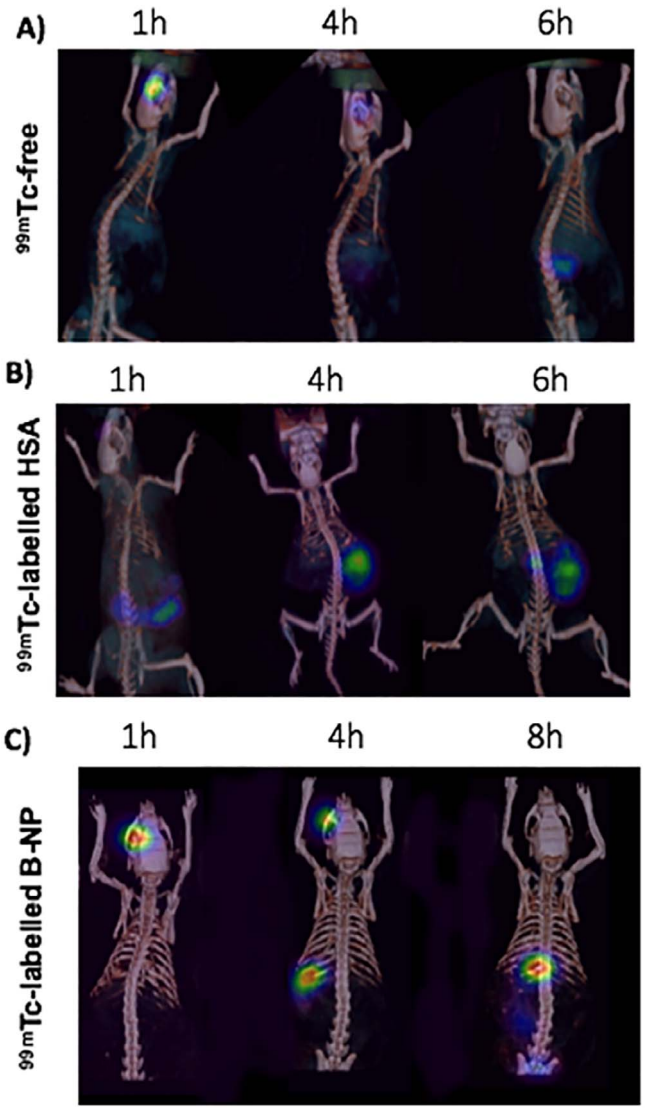

Fig. 11. (A) In vivo SPECT-CT images of ^{99m}Tc-free (upper row) compared with (B) ^{99m}Tc-HSA (medium row) and (C) ^{99m}Tc-B-NP (bottom row). Images in each row correspond to the same animal studied at the time points indicated in the figure. The intensity of images has been rescaled to the highest intensity point in each individual image to follow the transit of the radioactivity in the body of the animal.

when repeated doses were used on ARPE-19 cells viability assays. These results are in alignment with those previously published by other research groups, who described that bevacizumab did not affect the viability of different ocular cells (e.g., ARPE-19 and choroidal endothelial cells) either in normal or under oxidative stress conditions (Saenz-De-Viteri et al., 2016; Spitzer et al., 2007).

Finally, the biodistribution of these nanoparticles when administered as eye drops was evaluated in rats. Interestingly, bevacizumab-loaded nanoparticles remained in the eye for more than 4 h post-administration, while the control (HSA diluted in a commercial collyrium containing hydroxypropyl methylcellulose) appeared to be eliminated from the surface of the eye in less than 1 h. This finding of B-NP on the ocular surface agrees with other studies in which albumin nanoparticles show mucoadhesive properties when administered nasally (Luppi et al., 2011). The mucoadhesive behavior of these albumin nanoparticles would be a consequence of the establishment of links between nanoparticles and mucins through Van der Waals forces, electrostatic interactions and/or hydrogen bonds (Luppi et al., 2008).

In summary, bevacizumab-loaded albumin nanoparticles were produced by a desolvation procedure and subsequent freeze-drying. The resulting nanoparticles are stable without any supplementary stabilization process (e.g., cross-linkage with glutaraldehyde). This stability would be due to the development of protein-protein interactions between the antibody and albumin. These nanoparticles are not cytotoxic when evaluated in ARPE-19 cells. In addition, when administered as eye drops to laboratory animals they remain on the surface of the eyes for at least 4 h. All of these results evidence that these albumin-based nanoparticles may be good candidates for the ocular delivery of bevacizumab, opening the door to the evaluation of their efficacy in vivo.

Acknowledgements

This work was supported by the “Ministerio de Ciencia e Innovación“ (PRI-PIBAR-2011-1377) in Spain, by the ”Instituto de Salud Carlos III“ through the project NATERABEVA (PI14/01830, Spain) and by the ”Consejo Nacional de Investigaciones Científicas y Técnicas“ (CONICET) and the ”Secretaría de Ciencias y Tecnología-UNC) from Argentina.

References

Abrishamid, M., Ganavati, S.Z., Soroush, D., Rouhbakhsh, M., Jaafari, M.R., Malaekeh-Nikoueu, B., 2009. Preparation, characterization, and in vivo evaluation of nanoliposomes-encapsulated bevacizumab (Avastin) for intravitreal administration. Retina 29, 699–703.

Ahmed, M.H., Byrne, J.A., McLaughlin, J., Ahmed, W., 2013. Study of human serum albumin adsorption and conformational change on DLC and silicon doped DLC Using XPS and FTIR spectroscopy. J. Biomater. Nanobiotechnol. 4, 194–203.

Arevalo, J.F., Lasave, A.F., Wu, L., Maia, M., Diaz-Llopis, M., Alezzandrini, A.A., Brito, M., 2017. Intravitreal bevacizumab for proliferative diabetic retinopathy: results from the pan-American collaborative retina study Group (Pacores) at 24 months of follow-up. Retina 37, 334–343.

Battaglia, L., 2010. Solid lipid nanoparticles produced through a coacervation method. J. Microencapsul. 27, 78–85.

Bock, F., König, Y., Kruse, F., Baier, M., Cursiefen, C., 2008. Bevacizumab (Avastin) eye drops inhibit corneal neovascularization. Graefe’s Arch. Clin. Exp. Ophthalmol. 246, 281–284.

Bouyer, E., Mekhloufi, G., Rosilio, V., Grossiord, J.L., Agnely, F., 2012. Proteins, polysaccharides, and their complexes used as stabilizers for emulsions: alternatives to synthetic surfactants in the pharmaceutical field? Int. J. Pharm. 436, 359–378.

Campochiaro, P.A., 2013. Ocular neovascularization. J. Mol. Med. 91, 311–321.

Chang, J., Garg, N.K., Lunde, E., Han, K., Jain, S., Azar, D., 2012. Corneal neovascularization: an anti-VEGF therapy review. Surv. Ophthalmol. 57, 415–429.

Chappelow, A.V., Kaiser, P.K., 2008. Neovascular age-related macular degeneration: potential therapies. Drugs 68, 1029–1036.

Christiansen, C., Kryvi, H., Sontum, P.C., Skotland, T., 1994. Physical and biochemical characterization of Albunex, a new ultrasound contrast agent consisting of air-filled albumin microspheres suspended in a solution of human albumin. Biotechnol. Appl. Biochem. 19, 307–320.

Crisante, F., Francolini, I., Bellusci, M., Martinelli, A., D’Ilario, L., Piozzi, A., 2009. Antibiotic delivery polyurethanes containing albumin and polyallylamine nanoparticles. Eur. J. Pharm. Sci. 36, 555–564.

Desai, N., 2006. Increased antitumor activity, intratumor paclitaxel concentrations, and endothelial cell transport of cremophor-free, albumin-bound paclitaxel, ABI-007, compared with cremophor-based paclitaxel. Clin. Cancer Res. 12, 1317–1324.

Elzoghby, A.O., Helmy, M.W., Samy, W.M., Elgindy, N.A., 2013. Spray-dried casein-based micelles as a vehicle for solubilization and controlled delivery of flutamide: formulation, characterization, and in vivo pharmacokinetics. Eur. J. Pharm. Biopharm. 84, 487–496.

Fan, T., Yu, X., Shen, B., Sun, L., 2017. Peptide self-assembled nanostructures for drug delivery applications. J. Nanomater. 2017, 11–16.

Fasano, M., Curry, S., Terreno, E., Galliano, M., Fanali, G., Narciso, P., Notari, S., Ascenzi, P., 2005. The extraordinary ligand binding properties of human serum albumin. IUBMB Life 57, 787–796.

Ghuman, J., Zunszain, P.A., Petitpas, I., Bhattacharya, A.A., Otagiri, M., Curry, S., 2005. Structural basis of the drug-binding specificity of human serum albumin. J. Mol. Biol. 353, 38–52.

Gray, R., Bhattacharya, S., Bowden, C., Miller, K., Comis, R.L., 2009. Independent review of E2100: a phase III trial of bevacizumab plus paclitaxel versus paclitaxel in women with metastatic breast cancer. J. Clin. Oncol. 27, 4966–4972.

Green, M.R., Manikhas, G.M., Orlov, S., Afanasyev, B., Makhson, A.M., Bhar, P., Hawkins, M.J., 2006. Abraxane®, a novel Cremophor®-free, albumin-bound particle form of paclitaxel for the treatment of advanced non-small-cell lung cancer. Ann. Oncol. 17, 1263–1268.

Hawe, A., Friess, W., 2006. Physicochemical characterization of the freezing behavior of mannitol-human serum albumin formulations. AAPS PharmSciTech 7, 94.

Huppertz, T., de Kruif, C.G., 2008. Structure and stability of nanogel particles prepared by internal cross-linking of casein micelles. Int. Dairy J. 18, 556–565.

Ibrahim, N.K., Desai, N., Legha, S., Soon-Shiong, P., Theriault, R.L., Rivera, E., Esmaeli,

B., Ring, S.E., Bedikian, A., Hortobagyi, G.N., Ellerhorst, J.A., 2002. Phase I and pharmacokinetic study of ABI-007, a cremophor-free, protein-stabilized, nanoparticle formulation of paclitaxel. Clin. Cancer Res. 8, 1038–1044.
Kang, Y.N., Kim, H., Shin, W.S., Woo, G., Moon, T.W., 2003. Effect of disulfide bond reduction on bovine serum albumin-stabilized emulsion gel formed by microbial transglutaminase. J. Food Sci. 68, 2215–2220.
Kim, S.W., Ha, B.J., Kim, E.K., Tchah, H., Kim, T., 2008. The effect of topical bevacizumab on corneal neovascularization. Ophthalmology 115, e33–e38.
Kouchakzadeh, H., Shojaosadati, S.A., Shokri, F., 2014. Efficient loading and entrapment of tamoxifen in human serum albumin based nanoparticulate delivery system by a modified desolvation technique. Chem. Eng. Res. Des. 92, 1681–1692.
Kratz, F., 2008. Albumin as a drug carrier: design of prodrugs, drug conjugates and nanoparticles. J. Control. Release 132, 171–183.
Langer, K., Anhorn, M.G., Steinhauser, I., Dreis, S., Celebi, D., Schrickel, N., Faust, S., Vogel, V., 2008. Human serum albumin (HSA) nanoparticles: reproducibility of preparation process and kinetics of enzymatic degradation. Int. J. Pharm. 347, 109–117.
Li, F., Hurley, B., Liu, Y., Leonard, B., Griffith, M., 2012. Controlled release of bevacizumab through nanospheres for extended treatment of age-related macular degeneration. Open Ophthalmol. J. 6, 54–58.
Lopez, E.S., Ortiz, G.A., Potilinski, C., Croxatto, J.O., Gallo, J.E., 2017. Corneal neovascularization: a combined approach of bevacizumab and suramin showed increased antiangiogenic effect through downregulation of BFGF and P2X2. Curr. Eye Res. 21, 1–8.
Luppi, B., Bigucci, F., Cerchiara, T., Mandrioli, R., Di Pietra, A.M., Zecchi, V., 2008. New environmental sensitive system for colon-specific delivery of peptidic drugs. Int. J. Pharm. 358, 44–49.
Luppi, B., Bigucci, F., Corace, G., Delucca, A., Cerchiara, T., Sorrenti, M., Catenacci, L., Di Pietra, A.M., Zecchi, V., 2011. Albumin nanoparticles carrying cyclodextrins for nasal delivery of the anti-Alzheimer drug tacrine. Eur. J. Pharm. Sci. 44, 559–565.
McCormack, P.L., Keam, S.J., 2008. Bevacizumab: a review of its use in metastatic colorectal cancer. Drugs 68, 487–506.
McGregor, D., Bolt, H., Cogliano, V., Richter-Reichhelm, H.B., 2006. Formaldehyde and glutaraldehyde and nasal cytotoxicity: case study within the context of the 2006 IPCS human framework for the analysis of a cancer mode of action for humans. Crit. Rev. Toxicol. 36, 821–835.
Merodio, M., Arnedo, A., Renedo, M.J., Irache, J.M., 2001. Ganciclovir-loaded albumin nanoparticles: characterization and in vitro release properties. Eur. J. Pharm. Sci. 12, 251–259.
Niknejad, H., Mahmoudzadeh, R., 2015. Comparison of different crosslinking methods for preparation of docetaxel-loaded albumin nanoparticles. Iran. J. Pharm. Res. 14, 385–394.
Patil, G.V., 2003. Biopolymer albumin for diagnosis and in drug delivery. Drug Dev. Res. 58, 219–247.
Perren, T.J., Swart, A.M., Pfisterer, J., Ledermann, J.A., Pujade-Lauraine, E., Kristensen, G., Carey, M.S., Beale, P., Cervantes, A., Kurzeder, C., du Bois, A., Sehouli, J., Kimmig, R., Stähle, A., Collinson, F., Essapen, S., Gourley, C., Lortholary, A., Selle, F., Mirza, M.R., Leminen, A., Plante, M., Stark, D., Qian, W., Parmar, M.K.B., Oza, A.M., 2011. A phase 3 trial of bevacizumab in ovarian cancer. N. Engl. J. Med. 365, 2484–2496.
Qi, J., Yao, P., He, F., Yu, C., Huang, C., 2010. Nanoparticles with dextran/chitosan shell and BSA/chitosan core-Doxorubicin loading and delivery. Int. J. Pharm. 393, 177–185.
Sadaharu, M., Yu, I., Victor Tuan Giam, C., Hiroshi, W., Sumio, T., Toru, M., Masaki, O., 2004. Functional analysis of recombinant human serum albumin domains for pharmaceutical applications. Pharm. Res. 21, 1924–1932.
Saenz-De-Viteri, M., Fernández-Robredo, P., Hernández, M., Bezunartea, J., Reiter, N., Recalde, S., García-Layana, A., 2016. Single- and repeated-dose toxicity study of bevacizumab, ranibizumab, and aflibercept in ARPE-19 cells under normal and oxidative stress conditions. Biochem. Pharmacol. 103, 129–139.
Sánchez-Martínez, M., Da Costa Martins, R., Quincoces, G., Gamazo, C., Caicedo, C., Irache, J.M., Peñuelas, I., 2013. Radiolabeling and biodistribution studies of polymeric nanoparticles as adjuvants for ocular vaccination against brucellosis. Rev. Española Med. Nucl. e Imagen Mol. (English Ed) 32, 92–97.
Son, S., Song, S., Lee, S.J., Min, S., Kim, S.A., Yhee, J.Y., Huh, M.S., Chan Kwon, I., Jeong, S.Y., Byun, Y., Kim, S.H., Kim, K., 2013. Self-crosslinked human serum albumin nanocarriers for systemic delivery of polymerized siRNA to tumors. Biomaterials 34, 9475–9485.
Sousa, F., Cruz, A., Fonte, P., Pinto, I.M., Neves-Petersen, M.T., Sarmento, B., 2017. A new paradigm for antiangiogenic therapy through controlled release of bevacizumab from PLGA nanoparticles. Sci. Rep. 7, 3736.
Spitzer, M.S., Yoeruek, E., Sierra, A., Wallenfels-Thilo, B., Schraermeyer, U., Bartz-Schmidt, K., Szurman, P., Spitzer, B., 2007. Comparative antiproliferative and cytotoxic profile of bevacizumab (Avastin), pegaptanib (Macugen) and ranibizumab (Lucentis) on different ocular cells. Graefe's Arch. Clin. Exp. Ophthalmol. 245, 1837–1842.
Van Miller, J.P., Hermansky, S.J., Losco, P.E., Ballantyne, B., 2002. Chronic toxicity and oncogenicity study with glutaraldehyde dosed in the drinking water of Fischer 344 rats. Toxicology 175, 177–189.
Weber, C., Kreuter, J., Langer, K., 2000. Desolvation process and surface characteristics of HSA-nanoparticles. Int. J. Pharm. 196, 197–200.
Weiner, L.M., Surana, R., Wang, S., 2010. Antibodies and cancer therapy: versatile platforms for cancer immunotherapy. Nat. Rev. Immunol. 10, 317–327.
Wilson, B., Ambika, T.V., Dharmesh Kumar Patel, R., Jenita, J.L., Priyadarshini, S.R.B., 2012. Nanoparticles based on albumin: preparation, characterization and the use for 5-flurouracil delivery. Int. J. Biol. Macromol. 51, 874–878.
Yang, L., Cui, F., Cun, D., Tao, A., Shi, K., Lin, W., 2007. Pharmaceutical nanotechnology: preparation, characterization and biodistribution of the lactone form of 10-hydroxycamptothecin (HCPT)-loaded bovine serum albumin (BSA) nanoparticles. Int. J. Pharm. 340, 163–172.
Yang, F., Zhang, Y., Liang, H., 2014. Interactive association of drugs binding to human serum albumin. Int. J. Mol. Sci. 15, 3580–3595.
Yu, S., Hu, J., Pan, X., Yao, P., Jiang, M., 2006a. Stable and pH-sensitive nanogels prepared by self-assembly of chitosan and ovalbumin. Langmuir 22, 2754–2759.
Yu, S., Yao, P., Jiang, M., Zhang, G., 2006b. Nanogels prepared by self-assembly of oppositely charged globular proteins. Biopolymers 83, 148–158.
Zhang, S., Wang, G., Lin, X., Chatzinikolaidou, M., Jennissen, H.P., Laub, M., Uludağ, H., 2008. Polyethylenimine-coated albumin nanoparticles for BMP-2 delivery. Biotechnol. Prog. 24, 945–956.